The International Journal of Advanced Manufacturing Technology (2019) 105:2357–2367
https://doi.org/10.1007/s00170-019-04302-z

ORIGINAL ARTICLE

Manufacturing of sustainable ceramics with improved mechanical properties from hazardous car paint waste to prevent environment pollution

Vsévolod Mymrin[1] · Priscila B. Praxedes[1] · Kirill Alekseev[1] · Monica A. Avanci[1] · Paulo H. B. Rolim[1] · Ana E. Povaluk[1] · Yelaman K. Aibuldinov[2] · Rodrigo E. Catai[1]

Received: 9 July 2019 / Accepted: 13 August 2019 / Published online: 29 October 2019

Abstract
Paint waste sludge (PWS) is one of the most polluted wastes of automobile construction industry. The main objective of this study was the experimental control of the neutralization of hazardous PWS (up to 20 wt%) in kaolin clay composites during the sintering of their mixtures at temperatures of 1000 °C, 1050 °C, 1100 °C, 1150 °C, 1200 °C, 1250 °C, and 1300 °C in order to manufacture environmentally clean white ceramics. These raw materials and the developed ceramics were characterized by following methods: X-ray diffraction, X-ray fluorescence, atomic absorption spectroscopy, energy-dispersive spectroscopy, and laser micro-mass analyses. The flexural resistance of the ceramics reached 12.77 MPa, the linear shrinkage varied between − 3.32 and 11.29%, the water absorption values ranged between 1.61 and 3.02%, and the density diverged from 1.53 to 1.62 g/cm^3. These numbers significantly exceeded the values of the control samples without PWS during ceramics sintering at all temperatures. The decomposition of the crystalline structures of kaolin, gibbsite, muscovite, barite, and calcite was determined; instead, small amounts of mullite and cristobalite crystals with a high prevalence of glass-like amorphous material appeared. The values of the experimental leaching and solubility tests of heavy metals from the developed ceramics were significantly lower than those permitted by Brazilian standards. So, high values of mechanical and chemical properties of the developed ceramics permit to utilize PWS as valuable raw material for production of environmentally clean white bricks, blocks, and tiles and to decrease ecological damage of automobile industry.

Keywords Hazardous automobile paint waste · Kaolin clay · Mechanical property enhancement · Structure formation processes · Environmentally clean white ceramics

1 Introduction

The essential components of all solid wastes from the automobile industrial paint waste sludge (PWS) are solvents, resins, pigments, and additives. The wastes contain highly polluting heavy metals, such as cadmium sulfide, lead chromate, and other compounds with heavy metals; volatile organic compounds; and highly toxic gases [1]. Therefore, they are classified, according to Brazilian sanitary standards [2], as class I hazardous waste. Studies by the U.S. EPA [3] confirmed that "most PWS must be managed as hazardous waste." Rădoiu [4] presented a solution to the environment of Romania and the European for the recycling of PWS by burning in metallurgical processes. Rodríguez et al. [5] also considered the high-temperature process of Portland cement production an effective method of neutralizing high residue rates. The researchers [6] used PWS in concrete mixtures as a partial substitute for virgin latex. Petroleum waste can be included [7] in red ceramics to increase flexural resistance strength. Silveira et al. [8] added 10–40% of the PW of Brazil's General Motors to the components of the original blanket anti-noise and accomplished physical, thermal, and mechanical improvements. Silveira et al. [8] presented a new application of an already-introduced composite sustainability index that requires a minimum amount of data to monitor a sustainable chemical process.

✉ Vsévolod Mymrin
seva6219@gmail.com

[1] Federal University of Technology, Ecoville, 4900, Deputado Heitor de Alencar Furtado str., 4900, Campus Curitiba, Paraná 81280-340, Brazil

[2] Kazakh University of Technology and Business, Astana, Kazakhstan

Kaolin clay (KC) is traditionally used as a raw material for the production of porcelain, faience, refractories, and fine electrotechnical ceramics, as a filler in the production of paper, rubber, plastics, and bases for roofing materials. It is also part of pesticides and cosmetics products. The review [9] summarized some important research findings over the last 30 years based on kaolin or aluminosilicate-bearing industrial wastes and attempts to explain the chemistry and reaction mechanisms of the geopolymerization process for green cement and refractory production. In order to increase the efficiency of the KC's application for ceramic and filler for paper production, Saikia et al. [10] considered the possibility of cleaning it from common contaminants (quartz and siderite) by leaching with organic acids. Prior to the use of KC, El-Zahhar et al. [11] incorporated it into a polyacrylic acid for sorption of bromophenol blue dye. Natural KC was used [12] to prepare mesoporous silica for methylene blue absorption. In pursuance of improving the KC's absorption capacity, Aghaie et al. [13] developed a kinetic model to assess bioleaching of iron from kaolin [8]. Meroufel et al. [14] valuated the adsorption capacity of KC to remove Zn(II) heavy metal ion from aqueous solution.

The brief review of the literature on the use of the raw materials explored in this study shows the novelty of the developed compositions. The world's scientific literature does not contain any research information on ecologically clean composites from hazardous car paints and kaolin, with mechanical properties exceeding traditional white ceramics.

Therefore, the objectives of this research were as follows: (1) studying the possibility to apply hazardous PWS in composites with KC for the manufacture of white ceramics whose mechanical properties met the criteria established by Brazilian technical standards, (2) studying the physicochemical processes involved in the formation of ceramics structures during their sintering, and (3) developing new eco-friendly composites for ceramics production, using hazardous PWS to enhance the ceramics' mechanical and chemical properties.

2 Materials and methods

2.1 Experimental methods

The raw materials and ceramics were characterized using various methods. To study the chemical composition by the X-ray fluorescence (XRF) method, the Philips/Panalytical Spectrometer (model PW2400) was used. The powder method was performed using a Philips X-ray diffractometer (XRD), model PW1830, with a monochromatic wavelength λCu-Kα, at a 2 ° angle range of 2° to 70° to determine the mineralogical composition. The results of diffractogram patterns deciphering were performed with Super-Q X'Pert High Score software (database PDF-2). Morphological structures were obtained by FEI Quanta 200 LV scanning electron microscopy (SEM). Chemical micro-analyses were obtained using an Oxford (Penta FET-125 Precision) X-ACT EDS method and composition of isotopes by micro-mass analyses utilizing a laser micro-mass analyzer (LAMMA 1000, model X-ACT). The solubility and lixiviation of materials from liquid extracts were determined by atomic absorption spectrometry (AAS) with a Perkin Elmer 4100 spectrometer. The granulometric composition was checked through the analysis of particle size distribution by laser diffraction with a Granulometer CILAS 1064 (Brazil). The mechanical resistance of the test samples (TSs) was measured by the three-point flexural rupture strength (FS) method on an EMIC universal testing machine. The coefficient of water absorption by immersion—with an Instrutherm BD 200 linear shrinkage of TSs—using a digital caliper (DIGIMESS) was determined; specific gravity was determined after TS sintering at different temperatures.

2.2 Calculations

The flexural rupture strength of the sintered samples was calculated [15] using the following equation:

$$R_F = 3PL/bh^2 \quad (1)$$

where R_F is the flexural rupture strength (MPa), P is the maximum load supported by the specimen (N), L is the distance between the supports of the specimen (mm), b is the width of the sample (mm), and h is the height of the sample (mm).

The values of the water absorption coefficient (C_{WA}) of the TSs were calculated following NBR 15270-3 [15], using the following equation:

$$C_{WA} = [(M_{SAT} - M_D)/M_D] \times 100 \quad (2)$$

where M_{SAT} is the mass of the saturated specimen after 24 h in water and M_D is the mass of the specimen after oven-drying at 100 °C for 24 h.

The values for the bulk density (BD) were obtained from the following equation:

$$BD = P_s/V_s \quad (3)$$

where BD is the bulk density (g/cm^3), P_s is the mass of the sintered and dry TSs (g), and V_s is the volume of the sintered TSs (cm^3).

3 Characterizations of the raw materials

The automotive PWS in this study was collected from local industrial companies in the state of Paraná, Brazil; the KC sample was obtained from Farmanil Quima, Curitiba. KC

Table 1 Main oxides of the raw materials' chemical composition (by the XRF method)

	SiO_2	CaO	Al_2O_3	SO_3	Na_2O	K_2O	Fe_2O_3	TiO_2	P_2O_5	BaO	IL
PWS	7.5	10.3	0.5	3.5	0.2	nd	0.6	13.3	0.2	17.1	46.1
KC	45.1	nd	38.5	0.5	nd	0.4	0.3	< 0.1	< 0.1	nd	14.9

nd not detectable, *IL* ignition loss

was chosen due to the significant number of its deposits in Brazil and for aesthetic reasons. Besides, in the world's technical literature, there are no studies of composites from automotive paint waste with clays, in particular with kaolin.

3.1 Particle size distribution of the raw materials

The results of particle size distribution analysis by laser diffraction indicated that 10% of the PWS particles had diameters between 1 and 10 μm and that 60% of the particles exhibited diameters between 10 and 110 μm. Approximately 90% of the particles in potassium (K) presented diameters smaller than 20 μm, and nearly 50% had diameters of less than 2 μm. The PWS's sample was dark blue, almost black and oily, and almost hard with a bitumen-like appearance. This comparison was confirmed by its high gross calorific value (− 4328 kcal/kg).

3.2 Chemical composition of the raw materials

In order to study the PWS chemical composition (Table 1), the raw materials were at a temperature of 900 °C, and the minimal amount of ash obtained (8.8 wt%) was analyzed by XRF, which showed a high concentration of BaO (17.1%), TiO_2 (13.3%), CaO (10.3%), and SiO_2 (7.5%), with insignificant inclusions of other elements (Table 1). The extremely high calcination loss (CL = 46.07%) was due to the high content of organic components such as oil and various types of oily emulsions, paint, volatiles, and sulfur compounds with carbonate inclusions. It was also indicated the presence of SrO (0.2%), ZrO_2 (0.1%), and Br_2O, CuO, and ZnO, all of them in amounts < 0.1%.

Table 2 Results of the leaching and solubility tests of the PWS under study and of ceramics composition 7 after sintering at 1150 °C

	Leaching (mg/L)			Solubility (mg/L)		
	PWS	Comp. 7	NBR	PWS	Comp. 7	NBR
As	7.69	< 0.01	1.0	15.32	< 0.001	0.01
Ba	173.37	< 0.001	70.0	205.28	< 0.001	0.7
Cd	8.34	nd	0.5	18.27	nd	0.005
Pb	7.14	nd	1.0	11.96	nd	0.01
Cr	28.68	< 0.01	5.0	32.28	nd	0.05
Hg	3.21	nd	0.1	7.43	nd	0.001
Se	3.61	< 0.05	1.0	5.36	nd	0.01
Al	238.61	0.03	*	279.22	0.05	0.2
Cu	33.19	< 0.005	*	43.44	nd	2.0
Fe	23.34	< 0.05	*	53.31	< 0.05	0.3
Mn	29.54	0.01	*	85.25	0.04	0.1
Zn	69.35	< 0.002	*	89.35	< 0.002	5.0

Comp. 7 means composition 7 with the highest (20%) PWS content

*No restrictions in the Brazilian standards [2]

The leaching and solubility tests of the PWS's ash liquid extract by a more sensitive method, AAS, determined (Table 2) the presence of the following heavy metals: Sb < 50.0 mg/L, As < 50.0 mg/L, Ba − 283 mg/L, Be < 5.0 mg/L, Cd < 2.5 mg/L, Pb < 25.0 mg/L, Cl − 110.0 mg/L, Co − 22.0 mg/L, Cu − 114.3 mg/L, and Cr^{6+} − 2.5 mg/L. Almost all of these metal contents far exceeded the Brazilian sanitary standards [2]; therefore, PWS should be classified as hazardous waste.

KC showed the classical chemical composition; it consisted predominantly of SiO_2 (45.13%) and Al_2O_3 (38.58%), with the shallow incorporation of Fe_2O_3 (0.3%). The IL (14.98%) was due to the combustion of organic matter and to the moisture content.

3.3 Mineralogical compositions of the raw materials

The XRD pattern of the PWS's ash (Fig. 1a) indicated rutile TiO_2, barite $BaSO_4$, and calcite $CaCO_3$ with very high amorphous phase contents. The XRD of kaolin (Fig. 1b) revealed the following mineralogical compositions: kaolin $Al_4(Si_4O_{10})(OH)_8$, gibbsite $Al(OH)_3$, and muscovite $KAl_2(APWSi_3O_{10})(OH)_2$, with high amounts of amorphous materials. The compared raw materials differ sharply not only regarding the mineral composition of the crystalline phase but also in the number of amorphous materials. Thus, the maximum intensity of crystal peaks in the PWS sample exceeded only 225 counts per second (cps), while the intensities of the peaks in the KC sample surpassed 900 cps. The magnitude of the X-ray background (the distance between the base curve of the peaks and 0 cps of the schedule) was higher than most of the PWS peaks. In the KC diffractogram, on the contrary, the intensity of most of the crystal peaks went far beyond the height of the X-ray background. Such a comparison indicated a much larger content of amorphic phases in the PWS than in the KC samples.

3.4 Morphological structure of kaolin clay and paint waste mix

SEM images of KC and paint waste initial dry mix of composition 6 (Fig. 2a, b) showed the morphology of the particles with different sizes, shapes, edges, and angles and several

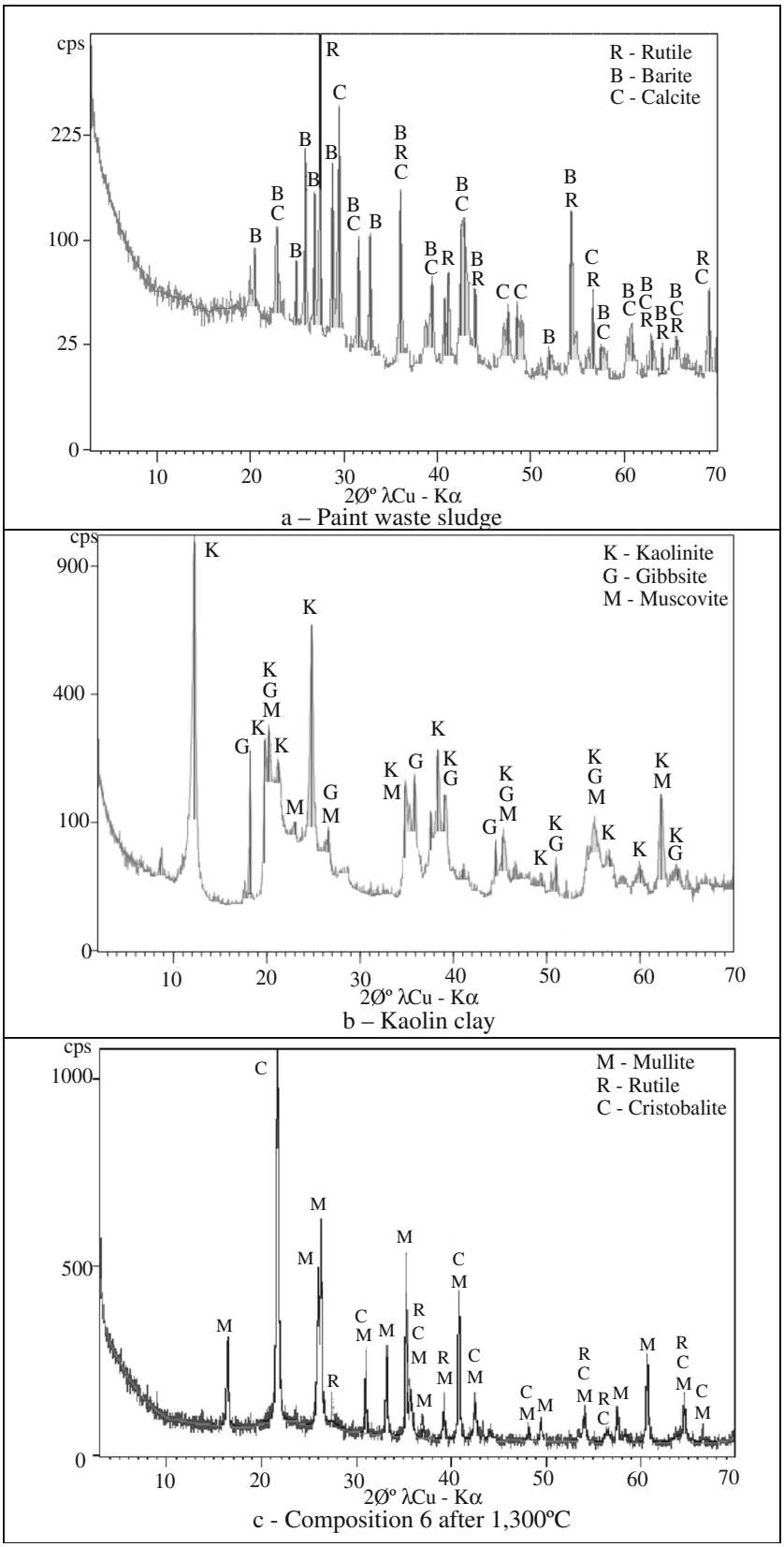

Fig. 1 Diffractogram patterns of paint waste sludge (PWS) (**a**), kaolin clay (KC) (**b**) in comparison with composition 6 after sintering at 1300 °C (**c**). 2Θ° λCu-Kα

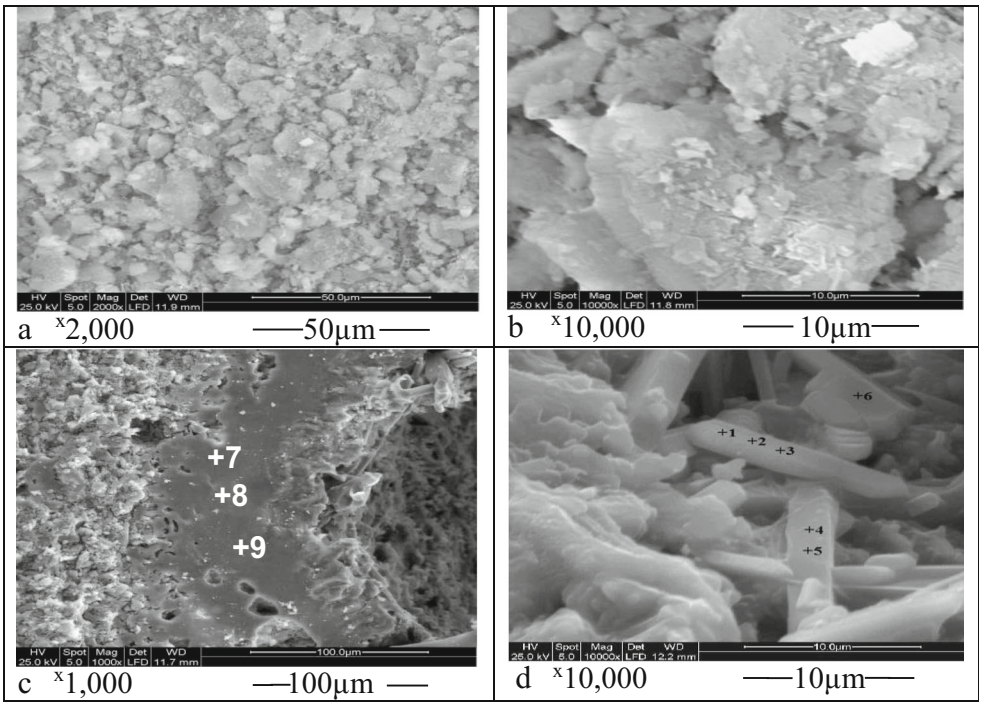

Fig. 2 SEM microstructures of composition 6 initial dry mix (**a**, **b**) and of the ceramic 6 sintered at 1300 °C (**c**, **d**) with the points of micro-chemical compositions by the EDS method. 100 μm

pores between them. Although these particles were not chemically interconnected, they can be adjusted mechanically.

3.5 TS preparation

The TSs of the materials were prepared by homogenizing the mixtures of raw materials manually at different percentages (Table 3). The TSs of composition 1 were prepared as control ceramics only with K, without the incorporation of PWS; the other composites were prepared by adding 2%, 4%, 8%, 12%, 16%, and 20% of PWS in the KC. The raw material mixtures were hydrated under optimum moisture (between 10 and 12%) and compacted at a pressure of 10 MPa in a rectangular mold with dimensions of 60 mm × 20 mm × 10 mm.

After drying in an electric oven at 105 °C to constant weight, the TSs were sintered (Fig. 3) for 6 h at 1000 °C, 1050 °C, 1100 °C, 1150 °C, 1200 °C, 1250 °C, and 1300 °C at a heating rate of 10 °C/min and were tested by the above methods. All mechanical property tests were performed with ten replicates, with calculation of averages and statistical deviations. Therefore, the total number of TSs was 490 pieces.

Table 3 Substantial composition of the ceramic's TSs

Components	Contents (wt%) of components in ceramics (no.)						
	1	2	3	4	5	6	7
PWS	0	2.0	4.0	8.0	12.0	16.0	20.0
K	100.0	98.0	96.0	92.0	88.0	84.0	80.0

4 Results and discussion

4.1 Physical properties of the ceramics

The following main physical properties of the developed ceramics were studied: flexural rupture strength, linear shrinkage, water absorption, and apparent density.

4.1.1 Flexural rupture strength of the ceramics

According to the Brazilian standard [15], the flexural rupture strength of the solid ceramics brick for masonry is classified as follows: class A, < 2.5 MPa; class B, 2.5–4.0 MPa; and class C, > 4.0 MPa. When burned at a temperature between 1000 and 1100 °C, all ceramics (Fig. 3) corresponded to class A; however, at 1150 °C, the resistance of ceramics 1 to 4 matched to class B standards, and that of ceramics 5–7 equated to class C (> 4.0 MPa). At the temperature of 1200 °C, all ceramics uniformly increased their resistance up to 7.18–10.39 MPa along with the crescent content of PWS. The control composition 1 (without PWS) exhibited the lowest resistance (7.04 MPa) among all. However, at the temperature of 1250 °C, this uniformity was disrupted by the resistance decrease of ceramic 4 (from 7.28 to 6.82 MPa), ceramic 5 (from 8.25 to 7.22 MPa), and ceramic 6 (from 9.47 to 9.18 MPa). After sintering at 1150 °C and higher, the resistance of control ceramic 1 remained the lowest (except T = 1250 °C) among all the developed materials. The highest strength value (12.77 MPa) was presented by ceramic 6, with 16% PWS content, after sintering at a temperature of 1300 °C, exceeding the

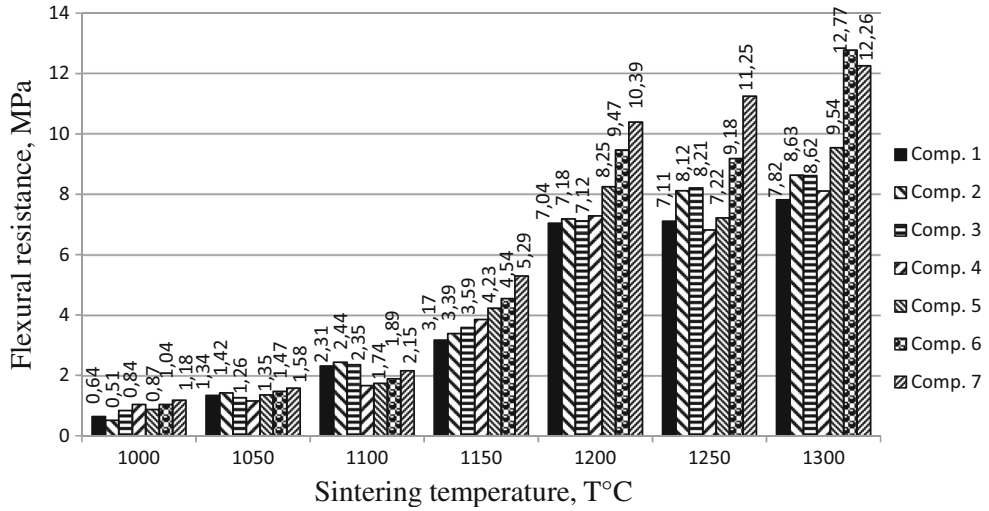

Fig. 3 Three-point flexural rupture strength of the ceramics sintered at different temperatures

requirements (4.0 MPa) of the class C technical standard by more than three times. This effect of the resistance enhancement of all the ceramics compared to the control TSs (composition 1) can be explained by the presence of substances such as heavy metals, emulsified oily components, paints, organic volatiles, sulfur compounds, carbonates, and other chemical and mineral impurities with relatively low melting or combustion temperatures in the PWS. This intensive sintering process caused the formation of a liquid phase due to the melting of fusible mineral impurities and chemical interactions with silica and alumina of the KC materials. At 1300 °C, the PWS acted as a flux with much higher efficiency than at 1150 °C.

Herek et al. [16] and Monteiro et al. [17] observed an inverse relationship—the decrease of the strength values with the increase of the sludge content during ceramics sintering. An explanation for this discrepancy in the results might be the significant difference in the chemical compositions of the raw components and the burning temperatures of their mixtures in the manufacture of ceramics. The leaching and solubility of metals, especially heavy metals, in the raw materials of both studies practically did not exceed the values of sanitary standards while the solubility of automotive paint waste far surpassed the permitted level of these standards for Hg (in 7430 times), Cd (in 3654 times), As (in 1532 times), Pb (in 1196 times), Cr (in 645.5 times), Ba (in 293 times), etc. All these metals played the role of fluxes so that increasing their content in the mixture

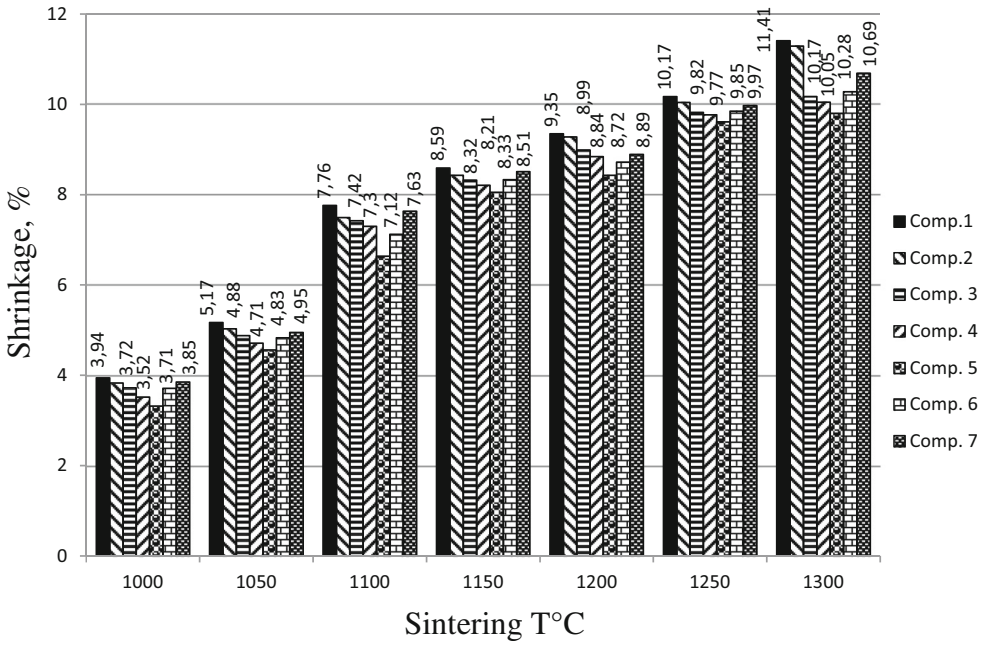

Fig. 4 Linear shrinkage of the ceramics after sintering at different temperatures

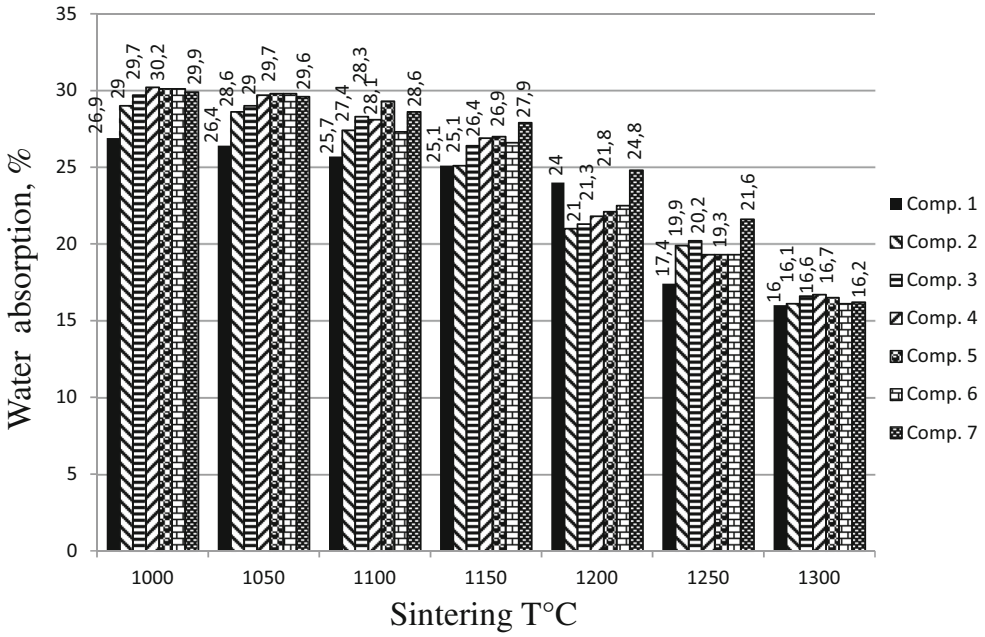

Fig. 5 Water absorption of the ceramics after sintering at different temperatures

raised the flexural strength and lowered the melting points of the blends. The sintering temperature of the comparative studies was no higher than 1000 °C, while the current studies were conducted within the range of 1000–1300 °C (Fig. 3).

The values of the flexural strength's standard deviation (Fig. 3) of all ceramics heightened with the increasing sintering temperature but did not exceed 5.2%.

4.1.2 Linear shrinkage of the ceramics

The ceramics showed (Fig. 4) an escalating linear shrinkage of the TSs with increasing sintering temperature. The shrinkage values of the control samples of the K (composition 1) were always higher than those of the ceramics with PWS.

This fact was also observed by Monteiro et al. [17]. The shrinkage values decreased with PWS contents up to 12%. However, with 16% and 20% PWS contents, they began to rise. This change was related to the increase in the degree of the material melting and the contraction of the molten phase, providing more heat-resistant solid particles of K.

Uncontaminated K (composition 1) and compositions 2–5, with PWS contents of 2–12%, exhibited less of the abovementioned fluxes; moreover, the fluxes were insufficient for the melting point of the volume of the TSs and its reduction.

The values of the standard deviation of the linear shrinkage coefficient after ceramic sintering at all temperatures varied between 0.18 and 1.43%.

4.1.3 Water absorption of the ceramics

The values of the water absorption coefficient (C_{WA}) were calculated using Eq. (2). The C_{WA} values (Fig. 5) rapidly declined with the increase in temperature for all developed ceramics. At all temperatures (except 1200 °C), the C_{WA} of the control composition was lower than the C_{WA} of the ceramics with different PWS contents. The overall trend was a slight gain in C_{WA} with the increase in PWS content, especially for composition 7, with 20% PWS content, after sintering at 1150–1250 °C. The main reason for this phenomenon was the growth in the gas formation due to numerous processes, such as structural water evaporation from crystalline structures of KC [kaolinite $Al_4(Si_4O_{10})(OH)_8$, gibbsite $Al(OH)_3$, and muscovite $KAl_2(AlSi_3O_{10})(OH)_2$], chemical interactions of the raw materials at high temperatures, and the burning of organic components.

In conformity with the Brazilian national standard [18], the ceramics after sintering at different temperatures are classified according to the water absorption in groups as follows: group Ia, between 0 and 0.5%; group Ib, between 0.5 and 3.0%; group IIa, between 3 and 6%; and group IIb, between 6 and 10%. Therefore, all developed ceramics can be classified as group Ib. Control ceramics prepared with composition 1, containing only kaolin clay sintered at 1000 °C, must be classified as belonging to group IIa. The standard deviation values of the water absorption coefficient of the ceramic for coating after sintering at all temperatures ranged between 0.03 and 0. 17%.

4.1.4 Bulk density of the ceramics

The apparent density of TSs (Table 4) was calculated using Eq. (3) as the ratio between the mass and apparent volume of the TSs. It was neatly visible (Table 4) that

Table 4 The bulk density of ceramics sintered at different temperatures

No.	Compositions (wt%)		Bulk density (g/cm^3) after sintering at different temperatures (°C)						
	PWS	Kaolin	1000 °C	1050 °C	1100 °C	1150 °C	1200 °C	1250 °C	1300 °C
1	0	100	1.57	1.56	1.55	1.53	1.53	1.52	1.52
2	2	98	1.57	1.57	1.56	1.56	1.56	1.56	1.57
3	4	96	1.56	1.56	1.57	1.57	1.58	1.58	1.60
4	8	92	1.60	1.59	1.58	1.59	1.61	1.62	1.64
5	12	88	1.62	1.62	1.61	1.60	1.62	1.63	1.65
6	16	84	1.65	1.64	1.63	1.64	1.65	1.67	1.69
7	20	80	1.68	1.67	1.66	1.67	1.68	1.69	1.72

there was a slow decrease in the bulk density of the control material (composition 1 with 100% of KC) from 1.56 g/cm^3 at 1000 °C till 1.52 g/cm^3 at 1300 °C. Adding 2% of PWS in composition 2 led to an even slower density's decrease from 1.57 g/cm^3 at 1000 °C till 1.56 g/cm^3 at 1250 °C, followed by its increasing till 1.57 g/cm^3 at 1300 °C. Density continually decreased with increasing temperature due to the burning of PWS's organic materials and fuel gas output. The yield of these gases with the mass loss of the TSs ceased in the temperature range of 1100–1150 °C, but the water absorption (Wa, Fig. 5) fell off and the increase in linear shrinkage (Fig. 4) of the samples remained steady. Evidently, this happened due to the melting process of PWS's metals, especially heavy metals with low melting points [19]. Doubling the PWS number till 4% (composition 3) caused an almost invariance of the density value at all temperatures at the level of 1.56 g/cm^3 at 1100 °C and its subsequent growth to 1.60 g/cm^3 at 1300 °C. Once more doubling of PWS until 8% (composition 4) caused a drop in the density from 1.60 to 1.58 g/cm^3 at 1100 °C followed by its growth to 1.64 g/cm^3 at 1300 °C.

The subsequent increase in PWS content by 4% each time (compositions 5–7) every time led to a decrease in density from 1100° or 1150° with its subsequent increase at 1300 °C. Thus, an increase in paint content by 2%, 4%, 8%, 12%, 16%, and 20% invariably escorted a rise in the ceramics' density by 0.01–0.05 g/cm^3 at 1300 °C.

4.2 Structure formation processes of the ceramics

4.2.1 Changes in mineralogical composition

It was determined, after the sintering of composition 6 at a temperature of 1300 °C, that the mineralogical composition of the ceramics consisted of (Fig. 1c) cristobalite SiO_2, mullite $3Al_2O_3{\cdot}2SiO_2$, and rutile TiO_2 with a very high content of amorphous phase. A comparison with the mineral composition of the raw materials (Fig. 1a, b) showed the disappearance after sintering of minerals of the PWS such as barite $BaSO_4$ and calcite $CaCO_3$ and of all K's minerals, namely kaolinite $Al_4(Si_4O_{10})(OH)_8$, gibbsite $Al(OH)_3$, and muscovite $KAl_2(AlSi_3O_{10})(OH)_2$. The crystal structures of cristobalite SiO_2 appeared instead of the SiO_2 of the decomposed K and the amorphous phases of both raw materials.

4.2.2 Changes in the morphological structure

The most representative SEM micrographs of the ceramics from composition 6, after sintering at 1300 °C for 6 h, demonstrated that the initially separated particles of different sizes and shapes (Fig. 2a, b) were transformed into a unified and continuous glassy material (Fig. 2c) with closed and open pores and a basically oval shape typical of melted materials. The micrographs also revealed crystal-like structures (Fig. 2d) of elongated shapes in druse-like clusters. Magnification at 10,000 times made the structures more visible and disclosed that they were not similar; some were elongated and thin, and others were flat and short. The distortion in shapes was probably caused by the fact that, upon cooling, these crystals failed to form completely due to the other crystalline structures near. There was not enough available space for these crystals to take on ideal shapes.

4.2.3 Chemical composition of new formations

The chemical composition of the ceramic's new formations was tested by EDS and LAMMA microanalysis. The content of each chemical element (Table 5) at points 7, 8, and 9, located in the visible glassy morphologies (Fig. 2c), was significantly altered and demonstrated an exceptional heterogeneity, typical of glass, e.g., K from 0.79 to 64.82%, Si from 0 to 12.08%, Al from 0 to 13.73%, and Fe from 0 to 19.08%, which would be impossible in true crystal structures. This finding indicated

Table 5 Chemical compositions of the new formations at the points shown in Fig. 2 c and d by EDS for ceramics 6 sintered at 1300 °C

Points	Contents of elements (wt%)										
	C	Al	Si	S	Cl	K	Ca	Ti	Fe	Ba	Total
1	41.37	12.15	22.16	5.15	1.50	0.11	6.26	6.75	3.23	1.32	100
2	27.03	11.10	20.86	0.54	–	2.03	15.46	19.40	0.25	3.33	100
3	45.16	10.73	23.60	–	1.63	0.74	9.19	7.39	1.22	0.34	100
4	35.29	24.15	32.03	1.27	–	0.82	1.33	1.55	0.53	3.03	100
5	51.81	21.59	14.04	0.20	2.08	6.60	0.34	–	3.34	–	100
6	27.29	24.43	34.14	1.23	3.01	2.89	0.56	6.45	–	–	100
7	6.60	13.73	12.08	0.23	2.09	64.82	0.45	–	–	–	100
8	41.04	–	0.26	0.72	10.23	3.25	24.18	8.47	11.85	–	100
9	54.84	0.21	–	0.57	12.86	0.79	0.17	8.39	18.60	3.57	100

that the new shapes, which were similar to real crystals, were amorphous formations.

The chemical compositions at points 1, 2, and 3 of the same crystal-like body presented considerable differences between the percent contents, analogous to the substantial divergence in the chemical compositions shown by the crystal-like shapes at points 4 and 5.

Equivalent results to SEM and EDS were obtained by LAMMA (Fig. 6) when testing the new ceramics' structures for composition 4.

The combinations of the isotopes with different relative atomic masses (ram) and their intensities (*I*, counts per second) were quite different at the ceramics' nearest points (A, B, and C). This fact confirmed the strong heterogeneity of the new ceramics' structures.

4.2.4 Environmental properties of the developed ceramics

The values of the experimental leaching and solubility tests were conducted on the samples of composition 7 because it had the maximum content of the polluted PWS (20%, Table 3) and the minimum content of the environmentally friendly component of the KC. The results of this study (Table 2), by the AAS method, demonstrated a robust decrease of leaching and solubility of heavy metals from ceramics 7 compared to PWS. Their relation to the requirements of the Brazilian standards [2] showed a significant advantage demonstrated by the obtained results. The leaching and solubility of some metals compared to PWS could reach a reduction of thousands of times: Ba, 173,370 and 205,280 times lower; Zn, 34,675 and 44,675 times lower; Cu, 6638 and 4344 times lower; and Cr, 2868 and 3228 times lower. These data indicated that the newly developed composites could be used as construction materials for tile and brick production. Furthermore, the use of these industrial wastes as raw materials could reduce the open quarry extraction of natural construction materials.

A similar effect of almost complete chemical bonding or encapsulation of heavy metals in ceramics was observed when using such highly polluted industrial wastes, copper-printed circuit board sludge, red mud of bauxite treatment and steel slag [20], and sewage sludge of municipal water treatment sludge [21].

The developed materials might be used for firing building materials such as bricks, tiles, pipes, and other construction materials; as a lining of low-temperature furnaces; fire retardant materials, etc. Their white coloring makes the color change of these materials easy, even with small amounts of tinted additives, significantly increasing their aesthetic attractiveness.

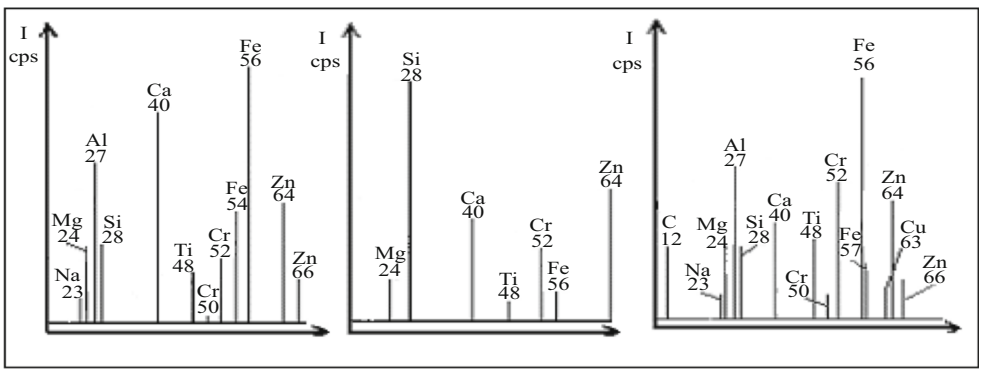

Fig. 6 Isotopes' micro-compositions of ceramic 6 after sintering at 1300 °C (by the LAMMA method)

Therefore, it was possible to state, based on the leaching/solubility results and the considerable technical literature, that the materials developed in this study could be successfully recycled as valuable components of new materials at the end of their useful life.

5 Conclusions

It was experimentally confirmed that the recycling of residual automobile paint waste in composites with natural kaolin clay could be used for the production of white ceramics. A sludge content of automotive paint waste of 20 wt% in the original blend provided a growth in the flexural strength of 63.8% compared to control samples, with a shrinkage reduction and minimal increases in bulk density and water absorption. Therefore, the introduction of this residue led to the enhancement of all ceramic properties in contrast to the control composition due to the presence of heavy metals, emulsified oily components, paints, and other chemical and mineral impurities with relatively low melting temperatures.

Physicochemical studies using a set of complementary methods revealed that during the composite sintering, minerals of the paint waste, such as barite $BaSO_4$, calcite $CaCO_3$, and all kaolin clay minerals, i.e., kaolinite $Al_4(Si_4O_{10})(OH)_8$, gibbsite $Al(OH)_3$, and muscovite $KA_{l2}(AlSi_3O_{10})(OH)_2$, were decomposed. Crystal structures of cristobalite SiO_2 appeared instead of SiO_2 from the kaolin and amorphous phases of both raw materials. Therefore, the mechanical properties of the developed ceramics can be explained by the synthesis of mainly amorphous glass-like structures with relatively small inclusions of some crystals of rutile TiO_2 and mullite $3Al_2O_3{\cdot}2SiO_2$.

Despite the high heavy metal content in the residual automobile paint waste, the leaching and solubility tests of the new ceramics showed that, during the sintering of the developed ceramics, all heavy metals were strongly chemically connected or securely capsulated in new glass formations. Therefore, the developed ceramics had leaching and solubility values hundreds of times lower than those permitted by Brazilian standards.

The extensive use of the method will have a positive impact on the environment by strong chemical bonding of hazardous heavy metals, by reducing the waste disposal and thus extending the useful life of industrial landfills and diminishing the exploitation of natural raw materials. These facts will serve as further evidence that the total utilization of industrial wastes as valuable raw materials is the best option of environmental policy.

The use of hazardous car paints and kaolin for obtaining eco-friendly composites whose mechanical properties exceed those of traditional white ceramics found no parallel in the world's scientific literature. The use of free waste as raw materials (or even with an additional payment from the producers of such waste to transport the residues produced) will always increase the economic efficiency of both enterprises, considering current land use taxes for expensive waste dumps and pollution fines.

Acknowledgments The authors are grateful to the staff of the Environmental Technology Laboratory (LTA) and the Laboratory of Minerals and Rocks (LAMIR), both from the Federal University of Paraná (Curitiba, Brazil), for their technical support of this research work.

References

1. Giudice CA, Pereyra AM (2009) Paints and coatings technology components, formulation, manufacturing and quality.1st edn. Edutecne; EBOOK, Buenos Aires http://www.edutecne.utn.edu.ar/tecn_pinturas/A-TecPin_I_a_V.pdf
2. NBR 10.004 (2004) Resíduos sólidos: Classificação. Rio de Janeiro. http://www.conhecer.org.br/download/RESIDUOS/leitura%20anexa%206.pdf
3. USA EPA (2006) Department of Toxic Substances Control Minimizing paint waste. 801. https://www.dtsc.ca.gov/PollutionPrevention/ABP/upload/TD_FS_Hazwaste.pdf
4. Rădoiu S (2007) Recycling possibilities for the wastes resulted from the paints and varnishes industry by pyrogenation. UPB Sci Bull 69:69–73
5. Rodríguez NH et al (2013) The effect of using thermally dried sewage sludge as an alternative fuel on Portland cement clinker production. J Cleaner Prod 52):94–102. https://doi.org/10.1016/j.jclepro.2013.02.026
6. Nehdi J, Sumner M (2003) Recycling waste latex paint in concrete. J Cem. Conc. Res. 33:857–863. https://doi.org/10.1016/S0008-8846(02)01084-0
7. Monteiro SN, Vieira CMF (2005) Effect of oily waste addition to clay ceramic. J Cer Int 31:353–358
8. Silveira R, de Verney Cézar J, Laranja R (2008) Ink sludge: solid residue reused in acoustic conditioning of Celta units in GMB – Gravataí, RS. J. SAE Technical Paper. 36:55. https://doi.org/10.4271/2008-36-0055
9. Liew YM et al (2011) Investigating the possibility of utilization of kaolin and the potential of metakaolin to produce green cement for construction purposes—a review. Australian J Basic and Appl Sci 5:441–449
10. Saikia NJ, Bharal DJ, Sengupta IP, Goswamee RL, Saikia PC (2003) Characterization, beneficiation and utilization of a kaolinite clay from Assam, India. J App Clay Sci 24:93–103. https://doi.org/10.1016/S0169-1317(03)00151-0
11. El-Zahhar AA, Awwad NS, El-Katori EE (2014) Removal of bromophenol blue dye from industrial waste water by synthesizing polymer-clay composite. J Mol Liq 199:454–461 https://doi.org/10.1016/j.molliq.2014.07.034
12. Shu Z, Li T, Znou J, Znou J et al (2014) Template-free preparation of mesoporous silica and alumina from natural kaolinite and their application in methylene blue adsorption. J Appl Clay Sci 102:33–40. https://doi.org/10.1016/j.clay.2014.10.006
13. Aghaie E, Pazouki M, Hosseini MR, Ranjba M (2012) Kinetic modeling of the bioleaching process of iron removal from kaolin. J Appl Clay Sci 65–66:43–47. https://doi.org/10.1016/j.clay.2012.04.011

14. Meroufel B, Benali O, Benyahia M, Zenasni MA, Merlin A, George B (2013) Removal of Zn (II) from aqueous solution onto kaolin by batch design. J Water Resource and Protection 5:669–680. https://doi.org/10.4236/jwarp.2013.57067
15. NBR 15270-3 (2005) Flexural rupture strength measurement and water adsorption measurements of ceramic bricks. Rio de Janeiro. https://www.abntcatalogo.com.br/norma.aspx?ID=588
16. Herek LC, Hori CE, Reis MHM et al (2012) Characterization of ceramic bricks incorporated with textile laundry sludge. J Cer Int 38:951–959
17. Monteiro SN, Vieira CMF, Ribeiro MM, Silva BAN (2007) Red ceramic industrial product incorporated with oil wastes. J Constr Build Mat 21:2007–2111
18. NBR 13817 (2009) Ceramic plates for coating. Rio de Janeiro. https://www.passeidireto.com/arquivo/17705810/nbr-13817-placas-ceramicas-pararevestimento-classificacao
19. Ribeiro MJ, Tulyaganov DU, Ferreira JM, Labrincha JA (2002) Recycling of Al-rich industrial sludge in refractory ceramic pressed bodies. J Ceram Int 28:319–326. https://doi.org/10.1016/S0272-8842(01)00097-9
20. Mymrin V, Guidolin MA, Klitzke W, Alekseev K, Guidolin RH, Avanci MA, Pawlowsky U, Winter E Jr, Catai RE (2017a) Environmentally clean ceramics from printed circuit board sludge, red mud of bauxite treatment and steel slag. J Cleaner Prod 164: 831–839. https://doi.org/10.1016/j.jclepro.2017.06.230
21. Mymrin V, Alekseev K, Fortini OM, Catai RE, Nagalli A, Rissardi JL, Molinetti A, Pedroso DE, Izzo RLS (2017b) Water cleaning sludge as principal component of composites to enhance mechanical properties of ecologically clean red ceramics. J Cleaner Production 145:367–373. https://doi.org/10.1016/j.jclepro.2016.12.141